Chapter 6

Scanning Electron Microscopy of Ctenophores: Illustrative Atlas

Tigran P. Norekian and Leonid L. Moroz

Abstract

Scanning electron microscopy (SEM) is a powerful tool for ultrastructural analyses of biological specimens at their surface. With comb jellies being very soft and full of water, many methodological difficulties limit their microanatomical studies via SEM. Here, we describe SEM protocols and approaches successfully tested on ctenophores *Pleurobrachia bachei* and *Beroe abyssicola*. Our SEM investigation revealed the astonishing diversity of ciliated structures in all major functional systems, different receptor types, and complex muscular architecture. These protocols can also be practical for various basal bilaterian lineages such as cnidarians.

Key words Ctenophora, Receptors, Neurons, Muscles, Digestive system, Cilia, *Pleurobrachia*, *Bolinopsis*, *Mnemiopsis*, Development, Evolution

1 Introduction

G. Adrian Horridge was the pioneer of electron microscopic investigation of ctenophores [1–6], with the first insights into the unique organization of these enigmatic animals and their nervous system. Mari-Luz Hernandez-Nicaise provided a further detailed ultrastructural analysis of ctenophore cells, neurons, and synapses [7–11]. These morphological and subsequent functional studies [12, 13] significantly contributed to the view that Ctenophora is a distinct lineage of early branching metazoans, sister to all other Metazoa [14–18]. Ctenophores might have developed muscular, neural, and other integrative systems independently from the rest of the animals [19–23]. Nevertheless, we know little about the identity and functions of many cell types and innovations within the ctenophore lineage. The ongoing single-cell transcriptomics in ctenophores [24] and future cell-type atlases should be inherently

Authors Tigran P. Norekian and Leonid L. Moroz have equally contributed to this chapter.

Leonid L. Moroz (ed.), *Ctenophores: Methods and Protocols*, Methods in Molecular Biology, vol. 2757,
https://doi.org/10.1007/978-1-0716-3642-8_6,

linked to the ultrastructural organization of particular cell populations.

Toward this goal, scanning electron microscopy (SEM) is a relatively fast and essential tool for higher-resolution imaging of virtually any structure. The resolution of electron microscopy is thousands of times higher than light microscopy for obvious reasons—the wavelength of electrons used for probing the tissue is much smaller than that of visible light (photons). There are two main challenges in SEM research, especially for fragile marine animals with high saltwater content: (1) vacuum and the need for dehydration and (2) creating the proper contrast. The beam of electrons in SEM must function in a relatively high vacuum, and therefore, any traces of evaporating water should be eliminated via complete dehydration of biological samples. This process of dehydration can easily destroy the surface structure of the tissue. Also, soft biological tissues are usually not sufficiently electron-dense and require additional techniques for creating a good contrast for visualization.

This chapter describes the SEM protocols for processing one of the most challenging animals for this technique—comb jellies. Ctenophores are composed of >95% water; therefore, fixation and dehydration usually cause significant tissue deformation. Nevertheless, we successfully adopted SEM protocols for both juvenile and adult stages of two ctenophore species: *Pleurobrachia bachei* and *Beroe abyssicola* (Fig. 1), which we describe here. These approaches revealed the astonishing diversity of ciliated structures, complex muscular architecture, rare mesogleal neurons, a variety of different receptor types, and other unique structures (*see* Figs. 2, 3, 4, 5, 6, 7, 8, 9, 10, 11, 12, 13, 14, 15, 16, 17, 18 and 19). Additional details can be found elsewhere [25–27]. These protocols can also be practical for various basal bilaterian lineages such as cnidarians [28].

2 Materials

1. High Mg^{2+} seawater—333 mM magnesium chloride was added to filtered seawater at 1:1 ratio.
2. Phosphate-buffered saline (PBS)—0.2 M stock solution, pH = 7.6.
3. Sodium bicarbonate 2.5% solution.
4. Cacodylate buffer—0.2 M stock solution, pH = 7.4, prepared from sodium cacodylate in distilled water with added HCl for pH balance.

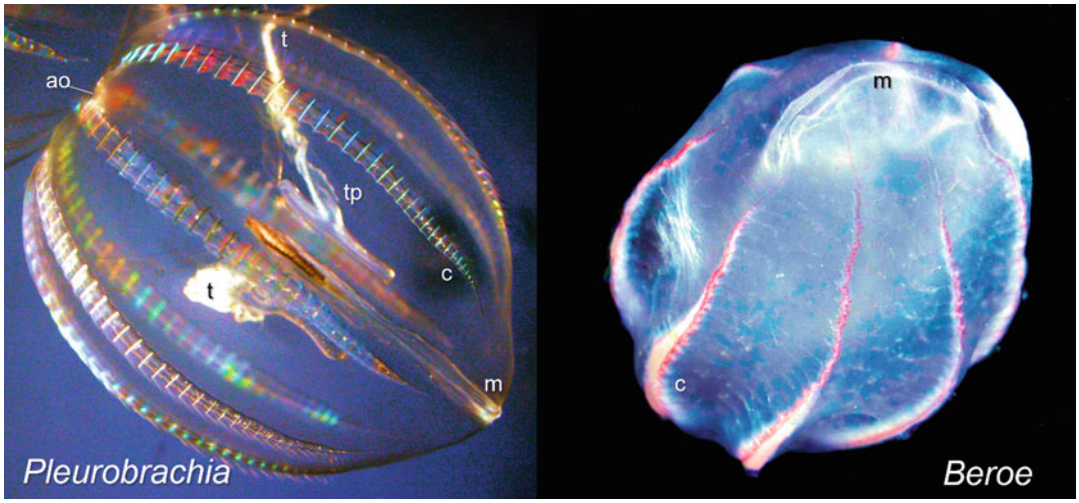

Fig. 1 *Pleurobrachia bachei* and *Beroe abyssicola* images with main organs. Abbreviations: *ao* the aboral organ, *m* mouth, *c* comb plates, *t* tentacles, *tp* tentacle pocket

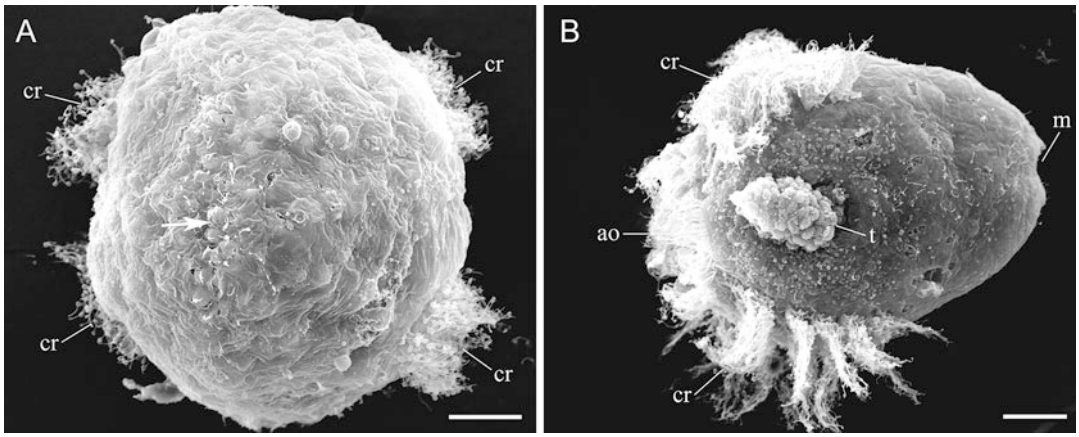

Fig. 2 *Pleurobrachia* embryos (SEM). (**a**) One-day-old embryo extracted from the egg capsule. Note that there are no tentacles outside the body, and the mouth is closed (arrow). (**b**) Three-day-old hatched larva with tentacles (*t*) and opened the mouth (*m*). Note also that there are only four ciliated rows (*cr*) in embryos (eight in adults, Fig. 1a). Scale bars: 20 μm

5. Glutaraldehyde—8% aqueous stock solution in 10 mL ampules, EM grade (Ted Pella, Catalog # 18421). The working concentration—2.5% glutaraldehyde in 0.1 M PBS.
6. Osmium tetroxide—4% aqueous stock solution in 5 mL ampules, EM grade (Ted Pella, Catalog # 18463). The working concentration—2% osmium tetroxide in 1.25% sodium bicarbonate.
7. Ethanol—100% solution.

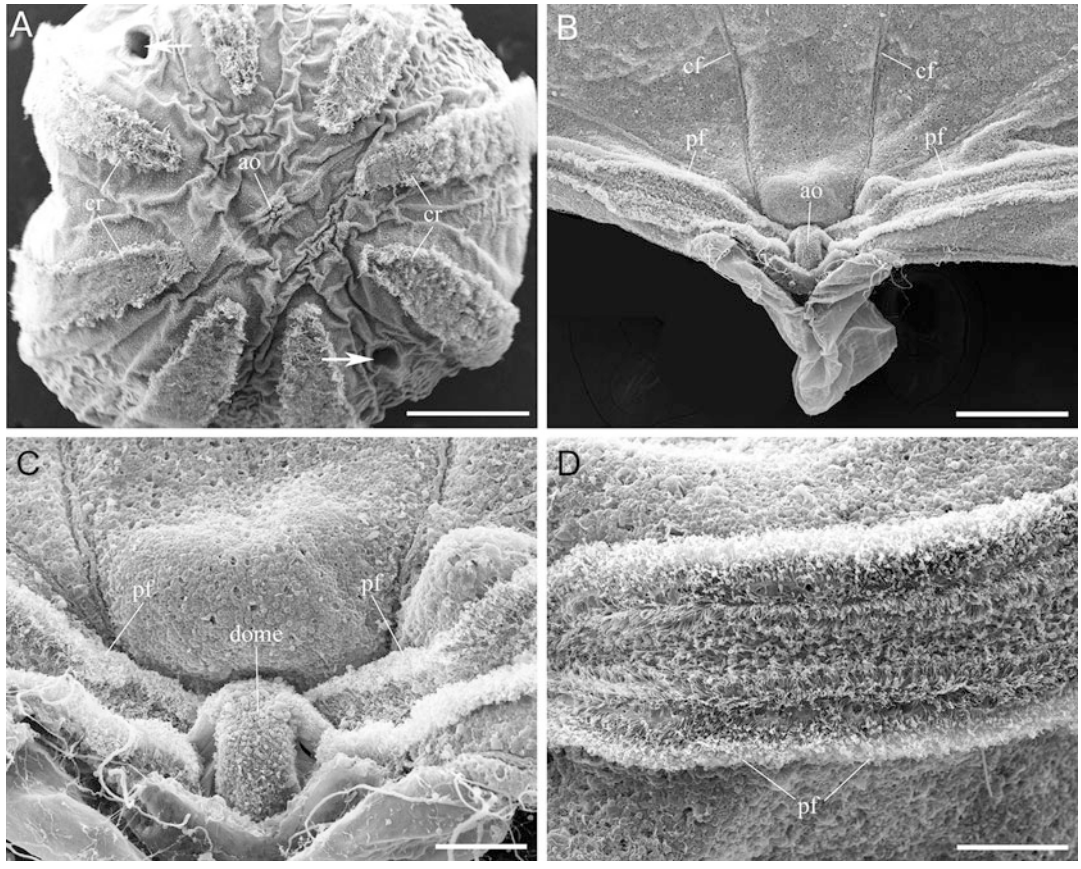

Fig. 3 Adult *Pleurobrachia* from the aboral side. (**a**) The whole *Pleurobrachia* preserved after fixation shows some shrinkage but remains mostly intact. Comb rows (*cr*) and aboral organ (*ao*) are clearly visible. Arrows point to the openings of the tentacle pockets. (**b**, **c**) Aboral organ (*ao*) area with polar fields (*pf*). The cut across *Pleurobrachia* was made next to the aboral organ along the polar fields. Note also the ciliated furrows (*cf*) running from the aboral organ to the comb rows. The aboral organ is covered by a protective dome that consists of long cilia. (**d**) Polar field (*pf*) contains numerous short cilia. Scale bars: (**a**) 1 mm; (**b**) 200 μm; (**c**, **d**) 50 μm

8. Liquid CO_2 for critical point drying.
9. Platforms for SEM viewing and containers for them.

2.1 Equipment

1. Critical point dryer—Samdri-790 (Tousimis Research Corporation).
2. Metal coating—Sputter Coater (SPI Sputter).
3. SEM microscope NeoScope JCM-5000 (JEOL Ltd., Tokyo, Japan).

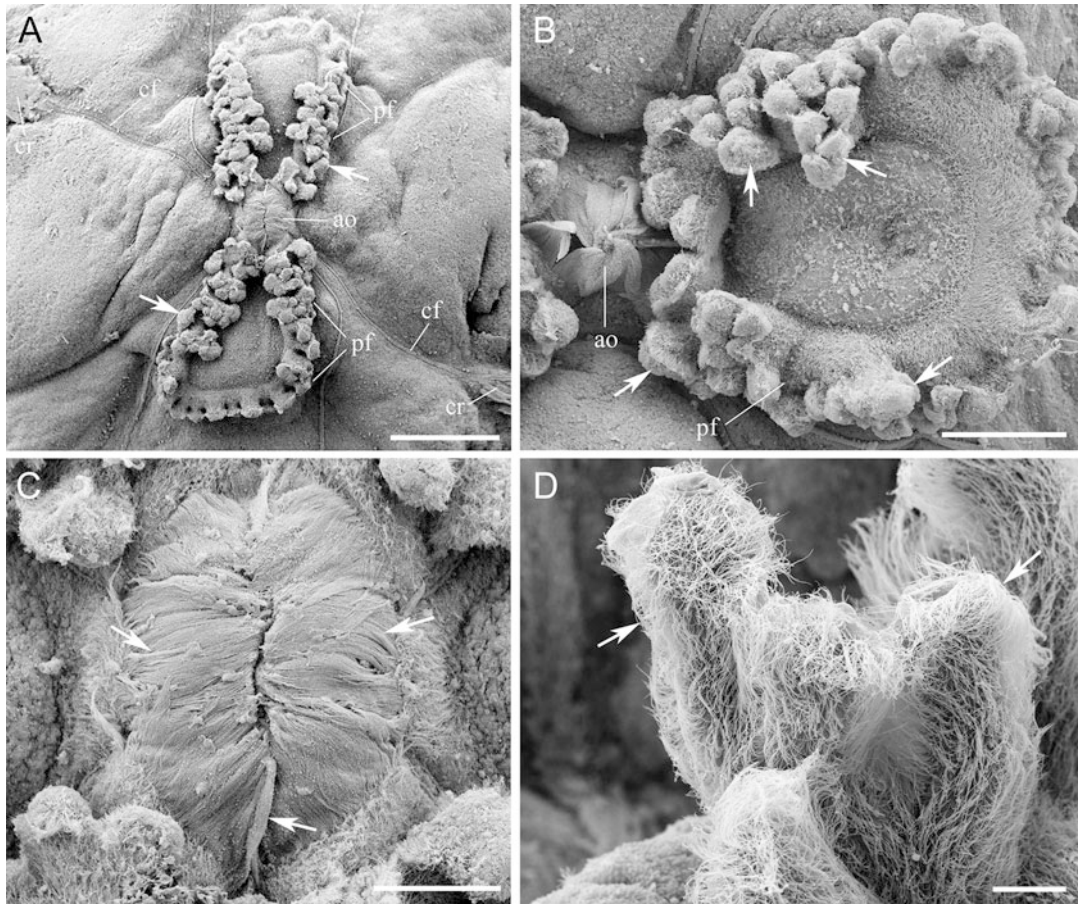

Fig. 4 Aboral organ and polar fields in adult *Beroe*. (**a**, **b**) Aboral organ (*ao*) and polar fields (*pf*) show proper, not withdrawn, shape after 1 h in high Mg^{2+} solution before fixation. Eight ciliated furrows (*cf*) are clearly visible, connecting the aboral organ with the comb rows (*cr*). Note that polar fields in *Beroe* have a crown of tall lobes (arrows) around their periphery. (**c**) The aboral organ is covered by a protective dome consisting of numerous long cilia (arrows). (**d**) The lobes (arrows) of polar fields are covered by long cilia. Scale bars: (**a**) 500 μm; (**b**) 200 μm; (**c**) 100 μm; (**d**) 20 μm

3 Methods

Primary fixation in glutaraldehyde—4 to 12 h

1. Before fixation, animals were incubated in high Mg^{2+} seawater (333 mM magnesium chloride was added to filtered seawater at 1:1 ratio) for about 1 h to completely relax the tissue and block any possible synaptic excitatory inputs to the muscle fibers. Otherwise, fixative caused strong muscle contraction in live ctenophores, withdrawal of some organs, and loss of natural and relaxed anatomical state. It was self-evident in more

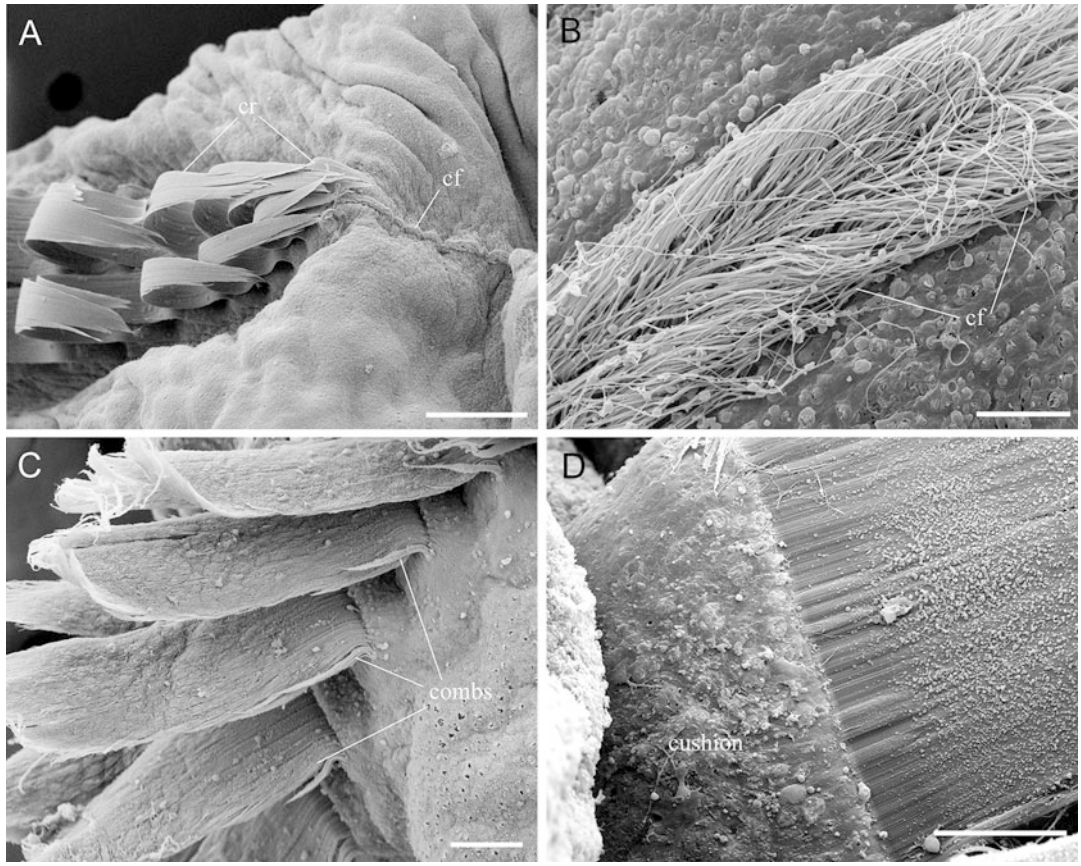

Fig. 5 Comb rows in adult *Beroe*. (**a**) Each comb row (*cr*) is connected to a ciliated furrow (*cf*). (**b**) Ciliated furrow (*cf*) represents a narrow band of tightly packed thin cilia. (**c**) Swim cilia arranged in rows of combs or ctenes. (**d**) At the base of each comb, there is a cushion consisting of polster cells that carry swim cilia. Scale bars: (**a**) 200 μm; (**b**) 10 μm; (**c**) 100 μm; (**d**) 50 μm

muscular *Beroe* compared to *Pleurobrachia*. For example, an aboral organ with polar fields in *Beroe* would be withdrawn entirely inside the body during fixation. Only prolonged high Mg^{2+} incubation beforehand would allow us to fix its proper anatomical state and view it on SEM.

2. After bathing in the high Mg^{2+} seawater, adult *Pleurobrachia* or small adult *Beroe* (0.5–5 cm long) were placed in 20–30 mL vials with closed lids.
3. The seawater was then removed from vials with a suction pipette, and 2.5% glutaraldehyde in 0.1 M phosphate-buffered saline (pH = 7.6) was immediately added (*see* **Notes 1** and **2**). The vials were then left for 4 h at room temperature or 12 h in a refrigerator at 5 °C.
4. Following fixation, the specimens were washed in 2.5% sodium bicarbonate solution. The fixative was removed from vials with

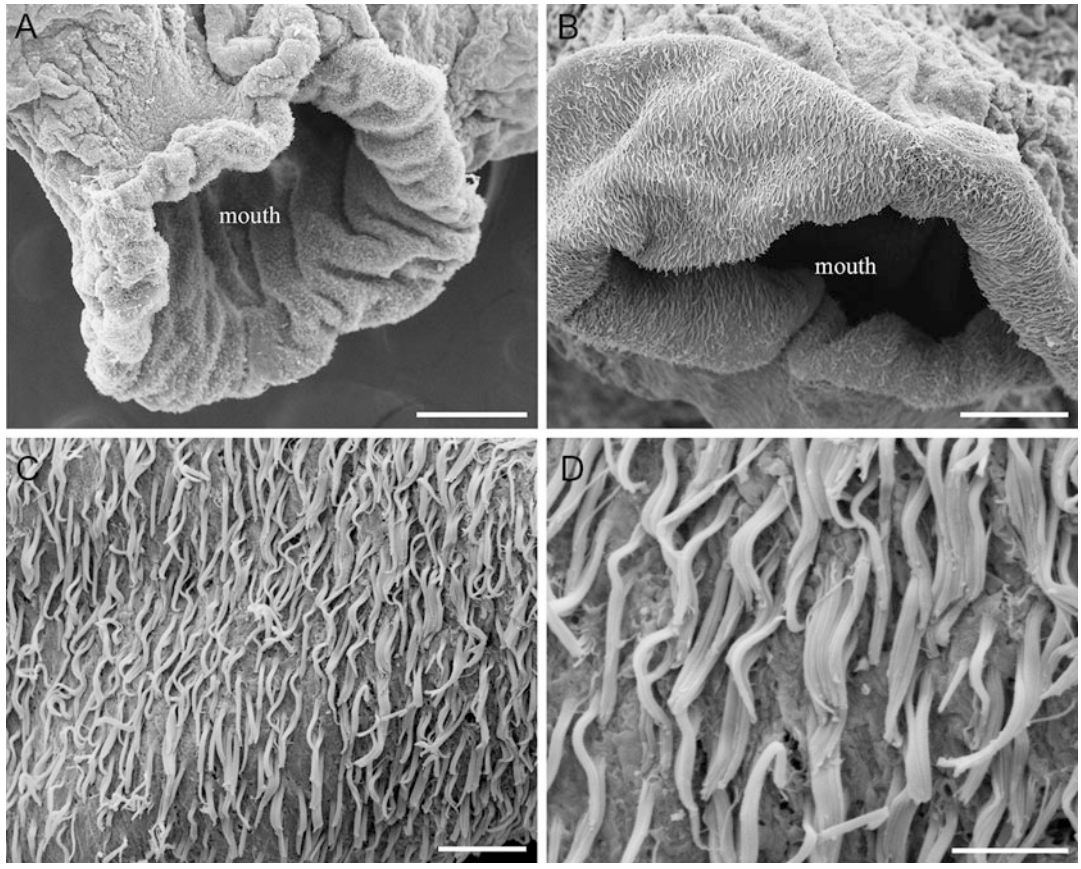

Fig. 6 Mouth area of adult *Pleurobrachia*. (**a**, **b**) Mouth shows significant shrinkage. (**c**, **d**) The inside surface of the lips is covered by cilia. Scale bars: (**a**) 200 μm; (**b**) 100 μm; (**c**) 20 μm; (**d**) 10 μm

suction pipettes and adequately disposed of—under the hood and with gloves. Then clean 2.5% sodium bicarbonate solution was added.

5. There should be at least three rinses in 2.5% sodium bicarbonate with a total wash time of 2 h. At this stage, the tissue can be stored in a refrigerator for a few days.

Secondary fixation in osmium tetroxide—3 to 4 h

6. Before the secondary fixation, the larger fixed animals were dissected and trimmed as necessary. The tissue was removed from the vials, placed in the small Petri dishes, and looked at under a dissecting microscope. The final size of the tissue should reflect the maximum field of view for the SEM—in our case, not more than 1 cm, and the anatomical functionality of dissected pieces. The smallest animals under 1 cm could be processed whole without dissection.

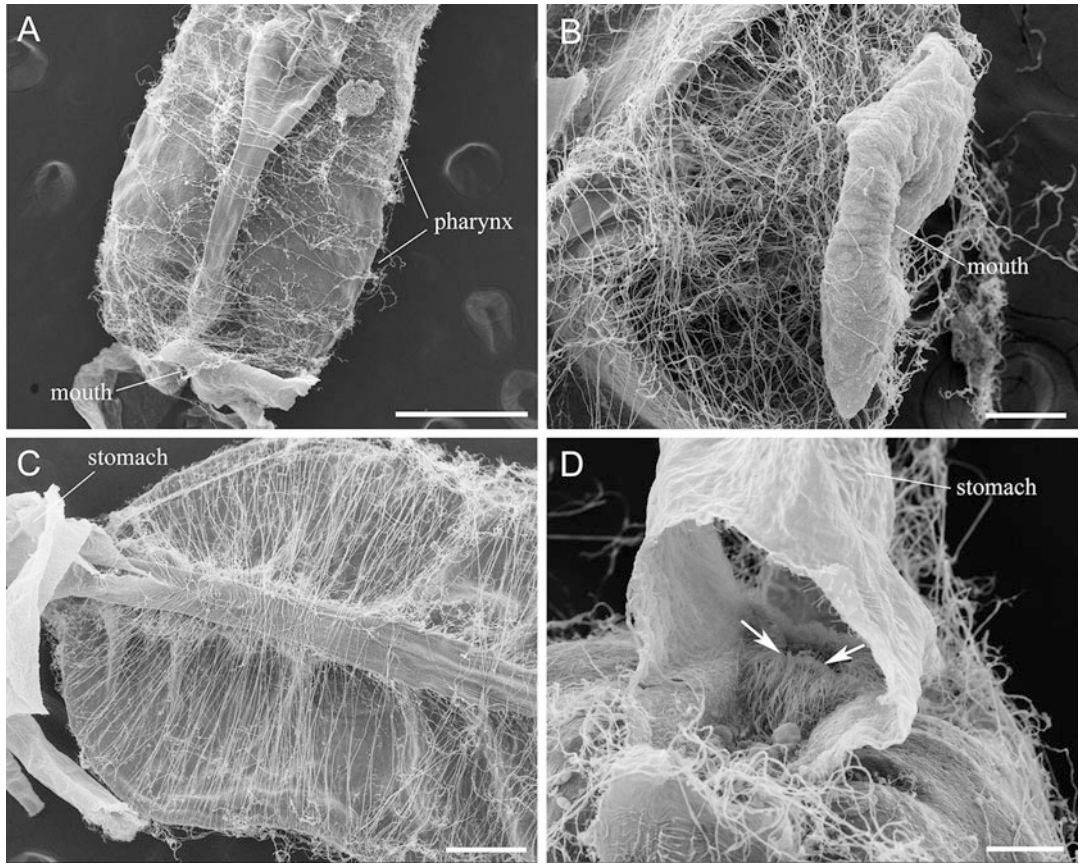

Fig. 7 Pharynx in *Pleurobrachia*. (**a**) Pharynx is frequently separated from the rest of the tissue during processing for SEM. (**b**) Mouth side of the pharynx with the lips still attached. (**c**) Stomach side of the pharynx. Note numerous thin, long muscle fibers that run through the mesogleal area and connect to the pharynx. (**d**) Pharynx and stomach are separated by a sphincter, which is densely covered with long cilia (arrows). Scale bars: (**a**) 500 μm; (**b**) 100 μm; (**c**) 200 μm; (**d**) 50 μm

7. The dissected pieces of tissue were then placed again in the 20–30 mL vials with the clean 2.5% sodium bicarbonate solution.
8. For secondary fixation, 2% osmium tetroxide in 1.25% sodium bicarbonate solution was added into the vials with ctenophore tissue. The vials were then left for 3 h at room temperature. The working solution of 2% osmium tetroxide should be prepared just before use—it does not last long, for a maximum of 2–3 days in a refrigerator. Osmium tetroxide is very toxic and should be handled carefully under the hood with gloves. The vials with tissue should be covered with a light-blocking container—osmium tetroxide is sensitive to light.

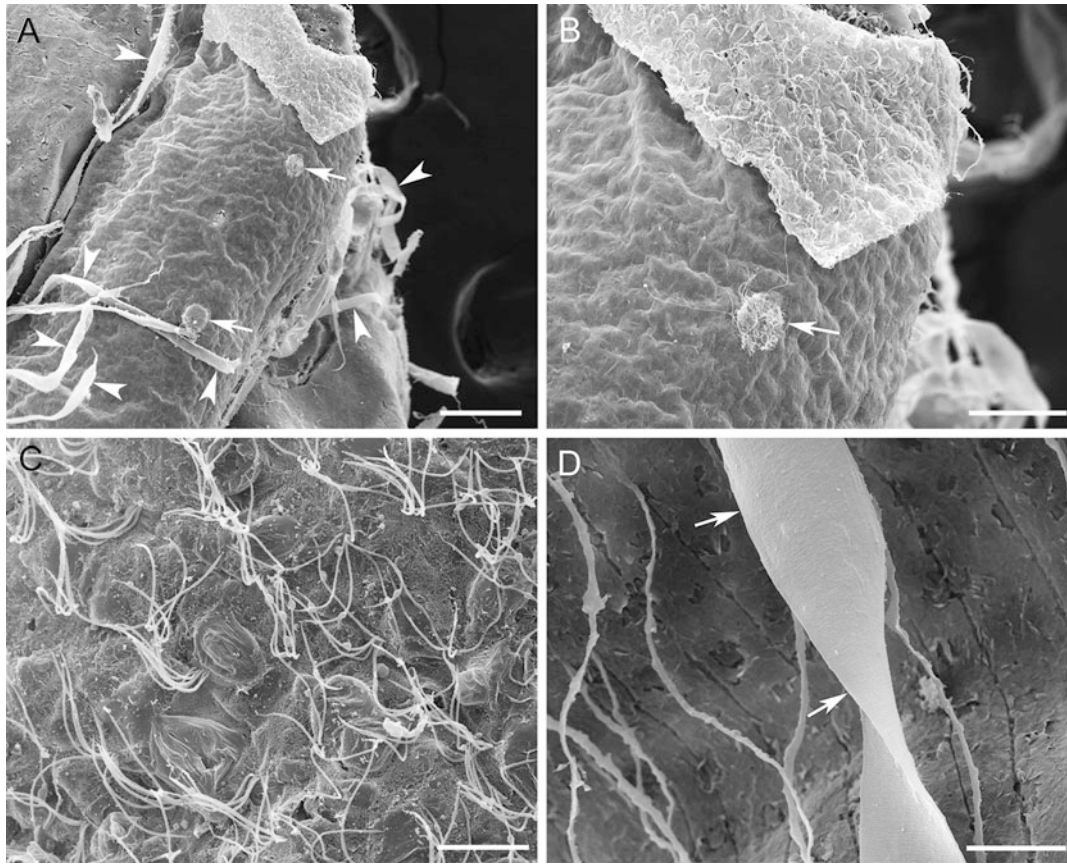

Fig. 8 Meridional canals in *Pleurobrachia*. (**a**, **b**) Meridional canals have pore complexes (ciliated rosettes) along their length, indicated by arrows. Arrowheads point to the long and flat muscle fibers connected to the body wall above the meridional canals along their entire length. Note that a strip of the meridional canal wall on the top of the image was flipped over to reveal its internal surface. (**c**) The internal surface of the meridional canal wall is covered with groups of long and flexible cilia. (**d**) Higher resolution image of a wide and flat long muscle fiber next to the meridional canal. Scale bars: (**a**) 100 μm; (**b**) 50 μm; (**c**) 10 μm; (**d**) 20 μm

9. After postfixation, osmium tetroxide should be appropriately disposed of, and the tissue should be rinsed several times with distilled water over 1 h.

Dehydration in ethanol—3 h

10. Next step was dehydration in ethanol. The dehydration series takes the tissue through the following ethanol concentrations: 30%, 50%, 70%, 90%, 100%, and second 100%. First, distilled water was removed with a suction pipette, and 30% ethanol was added to vials. Then 30% ethanol was removed, 50% ethanol was added, etc. Each step of incubation at a specific concentration should last about 30 min. Some shrinkage of the ctenophore tissue inevitably occurs during dehydration in ethanol

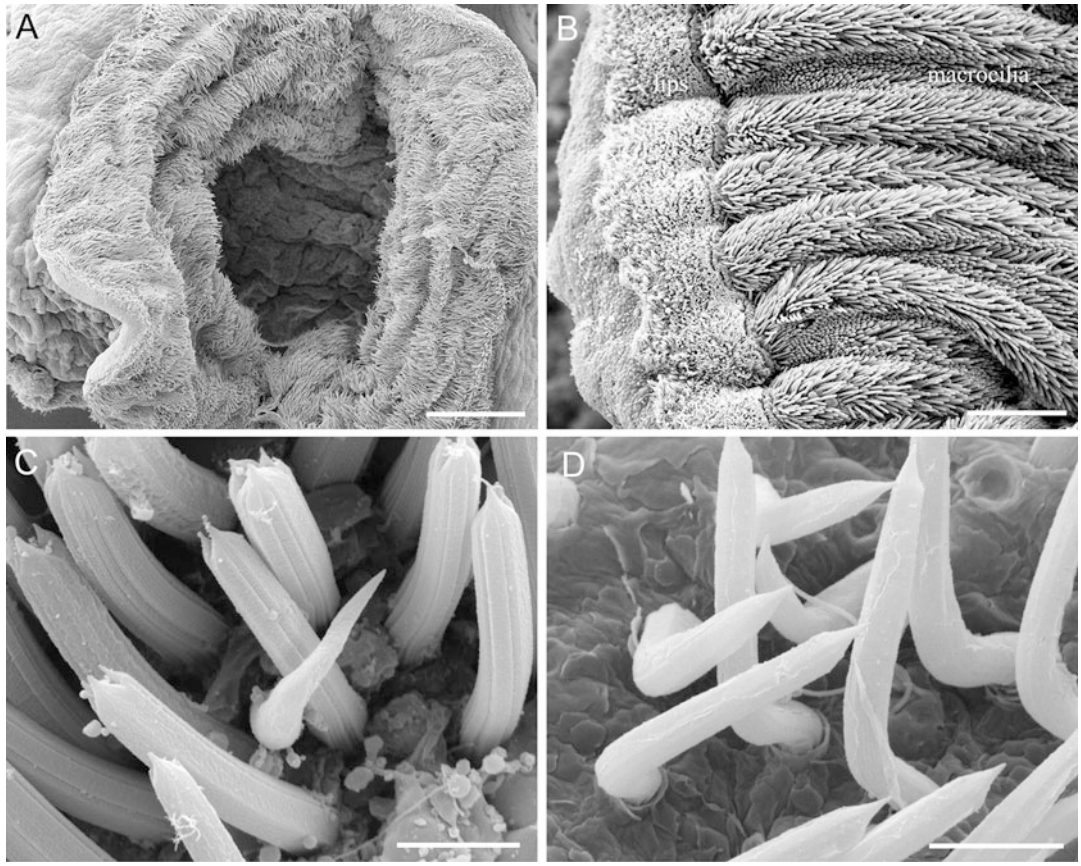

Fig. 9 Mouth of adult *Beroe* with macrocilia. (**a**) Opened mouth. (**b**) Macrocilia covers the entire area inside the mouth, from the lips to the entrance of the pharynx. (**c**) Closer to the lips, the macrocilia are always straight and display three sharp teeth at the end. (**d**) Further into the pharynx, the macrocilia density is reduced; they have a single sharp end and are usually bent like a hook pointing toward the inside of the pharynx. Scale bars: (**a**) 200 μm; (**b**) 100 μm; (**c**, **d**) 5 μm

(Figs. 6a, b and 9a). Also, the entire ctenophore or a large piece of tissue frequently breaks into smaller pieces at this stage. It happens because dehydration causes some loss of tissue flexibility, and tissue becomes more fragile, especially with areas that do not have dense and tough organs, such as ctene rows, pharynx, and tentacle pockets. This fact should not discourage us from proceeding further.

11. If there is a need to pause the protocol for a while, the best way to store specimens for a few days is in ethanol concentration of 70% in a refrigerator at 5 °C.

Critical point drying—2 h

12. The next step after dehydration was drying the tissue. The ctenophore specimens still in 100% ethanol were placed in a

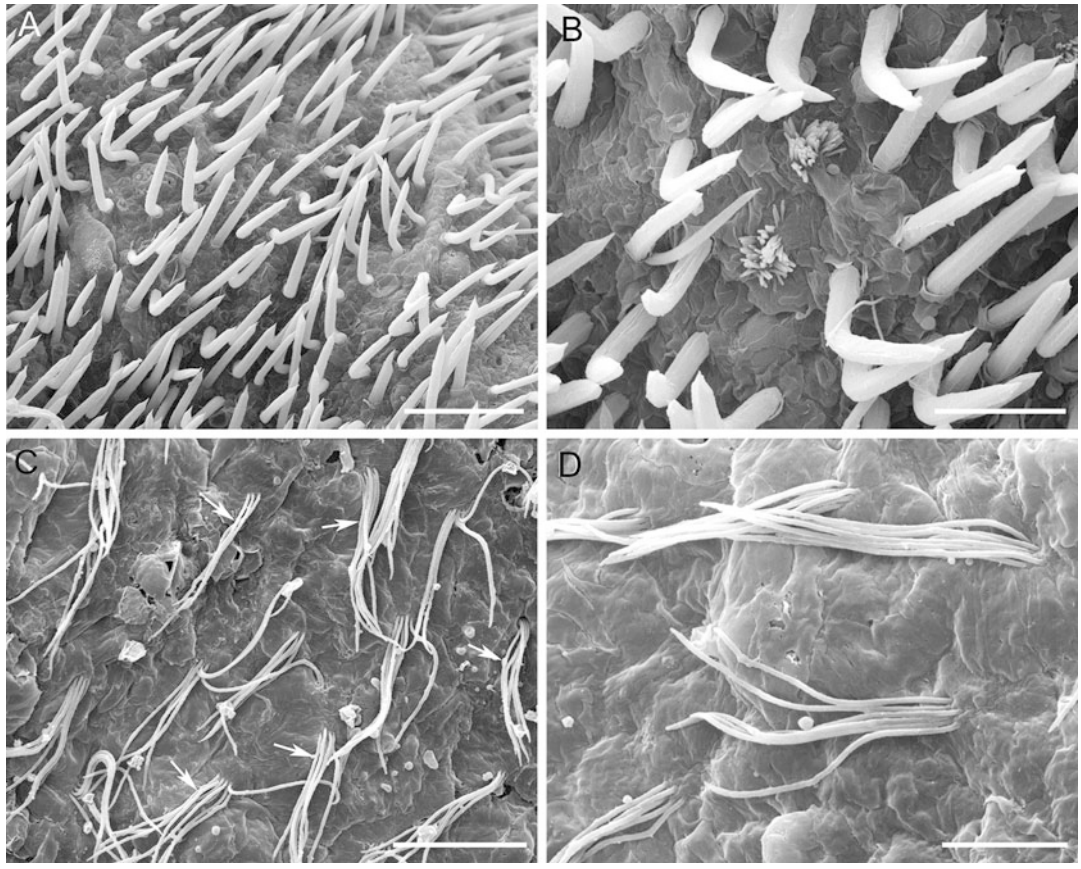

Fig. 10 Surface of the pharynx in adult *Beroe*. (**a**, **b**) Passing the mouth area and at the entrance of the pharynx, the macrocilia density is significantly reduced, and they become much shorter. (**c**, **d**) Further into the pharynx, macrocilia disappear entirely, and only groups of thin flexible cilia outline its surface. Scale bars: (**a**) 20 μm; (**b**, **c**) 10 μm; (**d**) 5 μm

critical point drying equipment chamber (*see* **Note 3**). We used mostly Samdri-790 dryer from Tousimis Research Corporation, but many different models are available on the market.

13. As a first step, ethanol should be replaced by liquid CO_2. It is important to ensure that all of the ethanol was replaced by CO_2. Depending on the thickness of the tissue and the number of specimens in the chamber, the duration of incubation in liquid CO_2 and the number of rinses should be increased. The samples will be ruined for good SEM imaging if some ethanol is left in the tissue. Usually, 30–40 min of incubation and 4–5 rinses were sufficient.
14. After passing the critical point, the liquid CO_2 evaporated during the drying procedure. For CO_2, the critical point is achieved at 35 °C and 1200 psi. Then the pressure was slowly

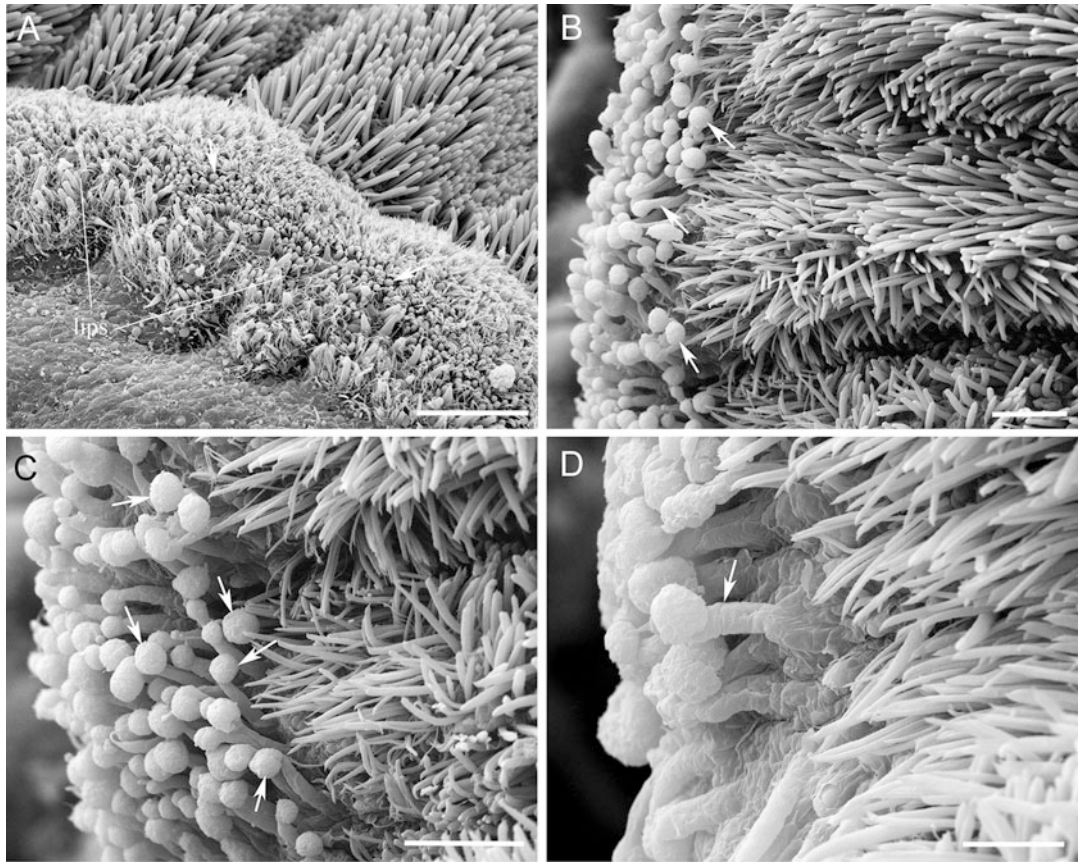

Fig. 11 The interlocking mechanism that keeps the lips closed in *Beroe*. In addition to adhesive epithelial cells, the lips contain numerous papillae-like structures (arrows), which mechanically fasten the lips together like a jigsaw puzzle. Some of the "locking" papillae are shorter than others and are spread over the entire lips area. Scale bars: (**a**) 50 μm; (**b**, **c**) 20 μm; (**d**) 10 μm

reduced to the atmospheric value. It was imperative to reduce it very slowly over at least 30 min.

15. The completely dry specimens were collected from the equipment chamber and placed under the dissecting scope for further refining. Additional breaking of original tissue could occur during critical point drying and some additional shrinkage. However, in some experiments, we managed to preserve a whole round-shaped body of *Pleurobrachia* for SEM imaging (Fig. 3a). In general, in highly muscular *Beroe*, the tissues did not go through as much breaking and shrinkage during the drying process as in other ctenophores, like *Pleurobrachia*.

Mounting tissue on viewing platforms—2 h

16. The tissue was placed on the holding platforms for SEM viewing during the next step. That was when the initial overview of

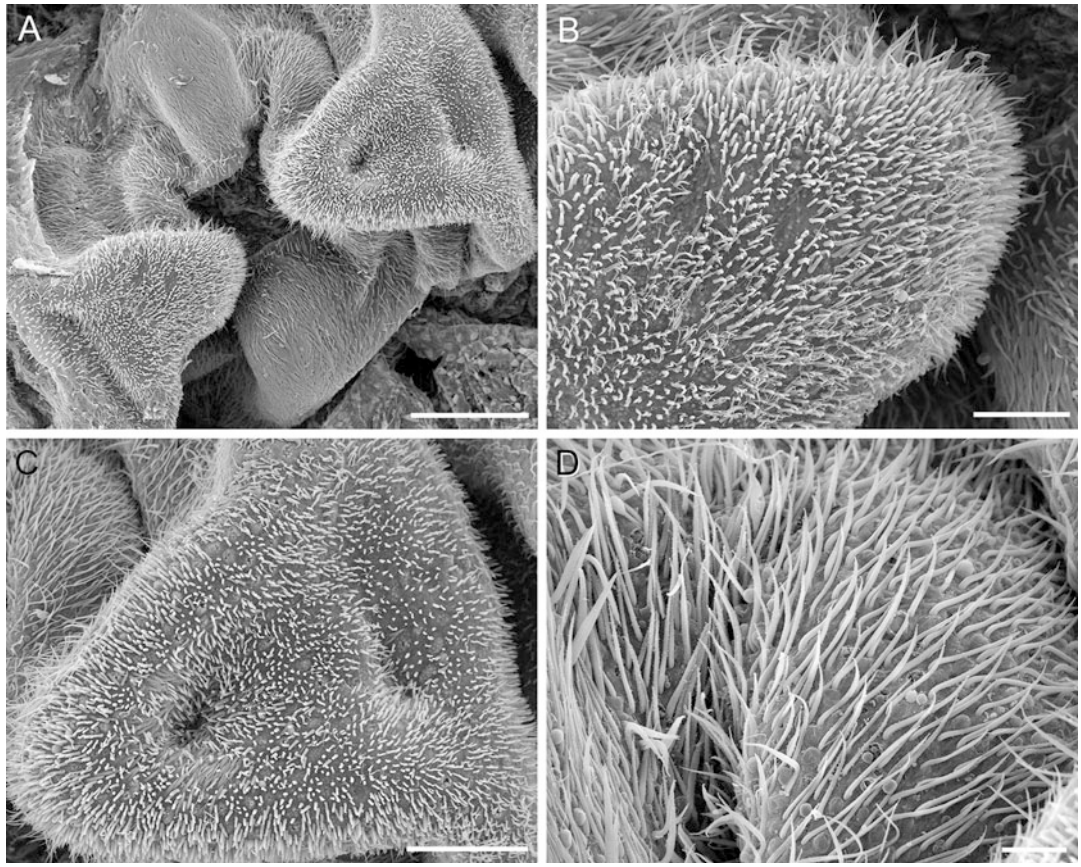

Fig. 12 The aboral end of the digestive system in *Beroe*. Note two symmetrical lobes and a highly ciliated surface. Scale bars: (**a**) 200 μm; (**b**) 50 μm; (**c**) 100 μm; (**d**) 20 μm

all dry samples occurred; the best pieces were selected for SEM viewing, carefully cleaned and dissected if necessary, and placed on the platform in a proper orientation. It should be done under a stereomicroscope using fine dissecting tools. At this stage, some dissecting can be done—for example, cutting open the tentacle pocket and revealing the withdrawn inside tentacles (Fig. 19d) or removing a piece of the integument and looking inside the mesogleal region at numerous muscle fibers attached to the pharynx of *Pleurobrachia* (Figs. 7 and 16), or mesogleal fibers attached to the outside wall of *Beroe* (Fig. 18).

Metal coating—1 h

17. Before inserting the platforms into SEM, the specimens should be processed for a metal coating to create a proper electron density on the surface and, therefore, good contrast for visualization. We used Sputter Coater from SPI Sputter. One crucial detail is that better metal coating leads to better imaging. So,

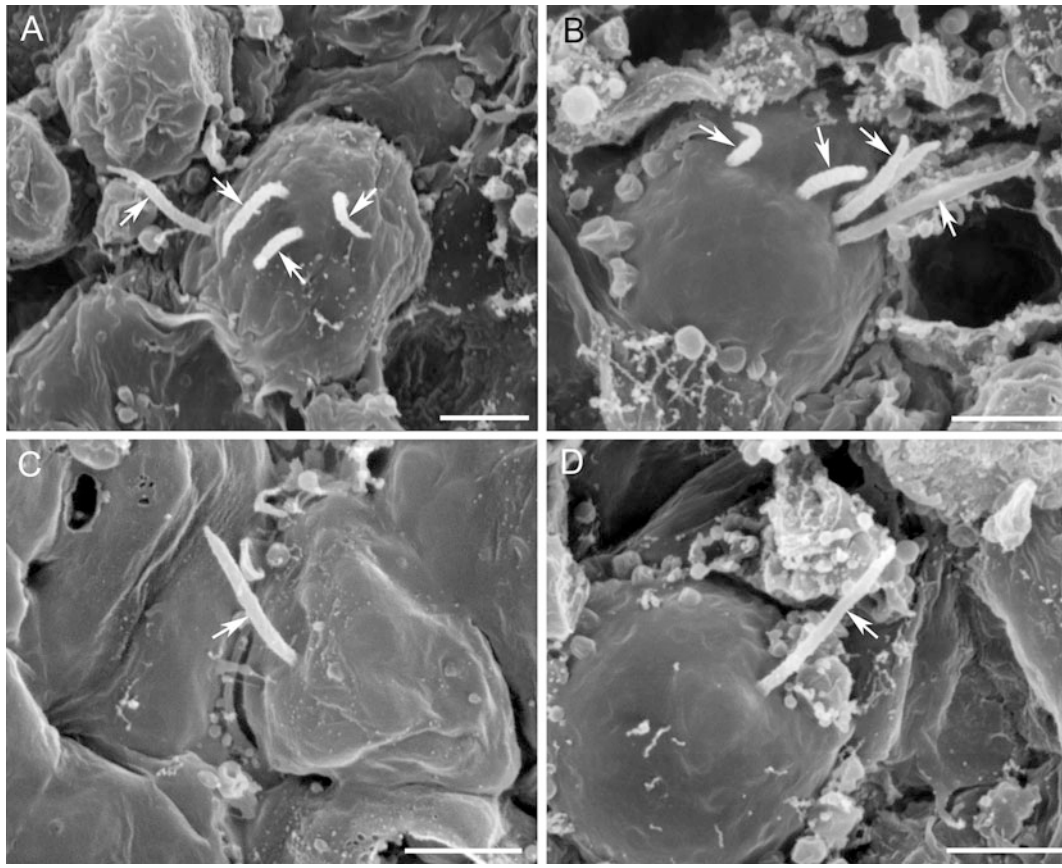

Fig. 13 Surface receptors in *Pleurobrachia*. (**a**, **b**) Receptors with multiple cilia. (**c**, **d**) Receptors with a single cilium. Arrows point to individual cilia. Scale bars: 2 μm

we ran the samples through metal coating twice, rotating the platforms 180° in between to ensure that tissue was covered at all angles.

SEM imaging

18. SEM observations and recordings were done on a portable, desktop SEM microscope NeoScope JCM-5000 (JEOL Ltd., Tokyo, Japan). It was straightforward to use, without additional cooling systems, and powerful enough for most biological purposes. Except for some tissue shrinkage, the preservation of the surface structure in *Pleurobrachia* and *Beroe* was very good and provided a lot of important information [25–27]. Excellent images were obtained from ciliated structures such as swim cilia (Fig. 5), sensory cells on the surface of the body (Figs. 13 and 14), macrocilia inside the mouth of *Beroe* (Figs. 9 and 10). We also had an interesting view of internal areas such as mesoglea with different internal

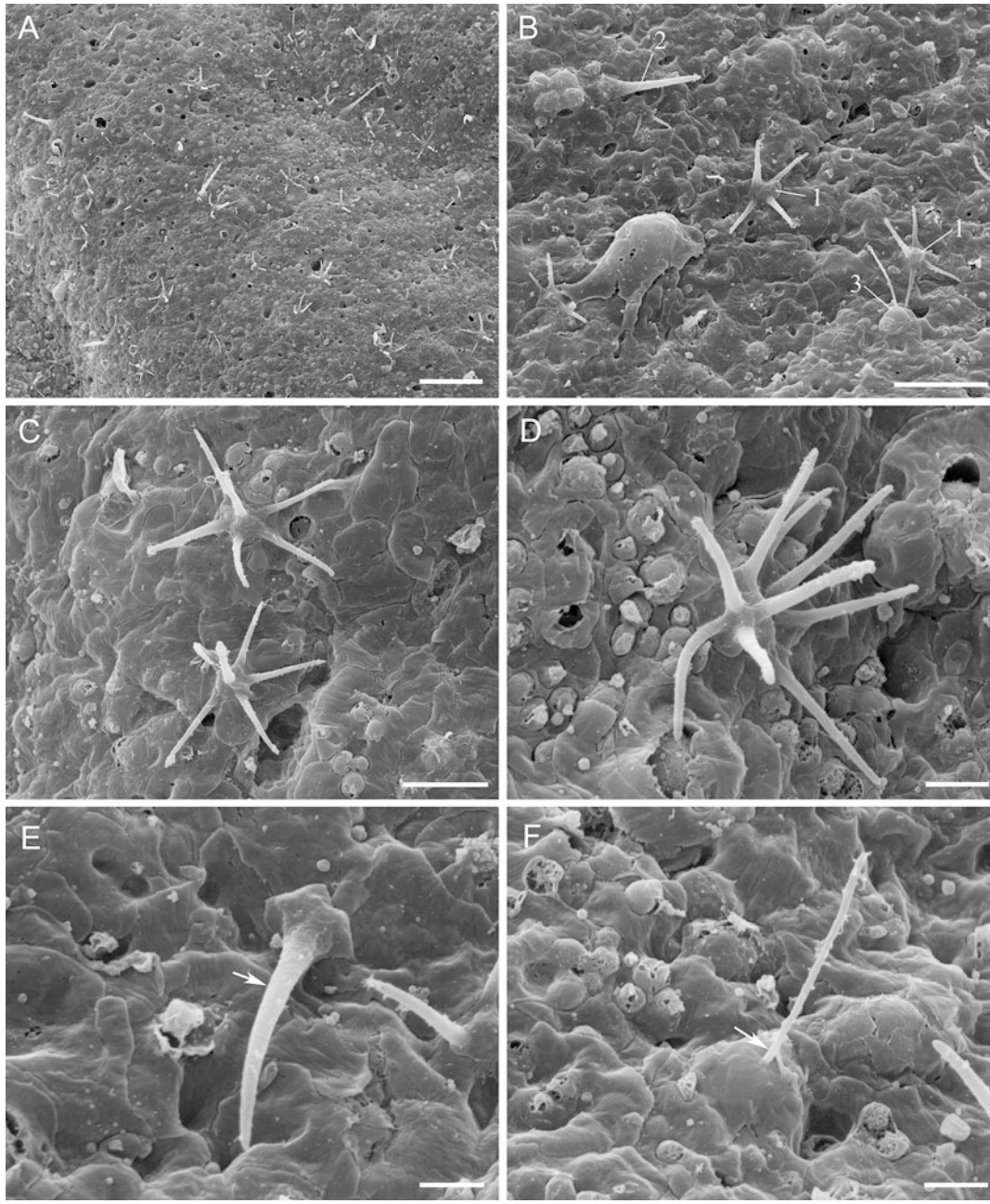

Fig. 14 Surface receptors in *Beroe*. (**a**) The surface of the body is covered with numerous ciliated receptors. (**b**) There are three types of receptors: receptors with multiple cilia (type *1*), receptors with a single large and thick cilium (type *2*), and receptors with a single thin cilium on the apical part of a cell (type *3*). (**c**, **d**) Type 3 receptor with a group of 3–9 cilia. (**e**) Type 2 receptor with a thick and long single cilium (arrow). (**f**) Type 3 receptor with a single thin and long cilium (arrow). Scale bars: (**a**) 20 μm; (**b**) 10 μm; (**c**) 5 μm; (**d**, **e**, **f**) 2 μm

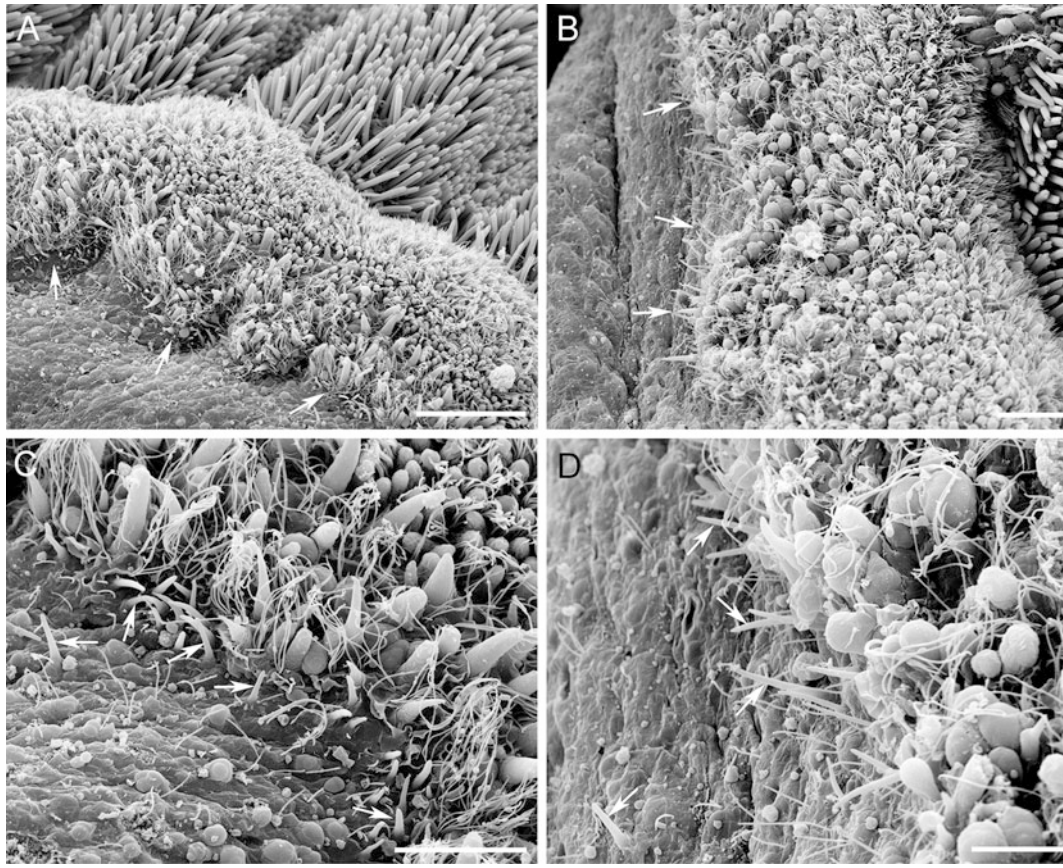

Fig. 15 Receptors on the edge of the mouth in *Beroe*. (**a**, **b**) The lips area contains numerous receptors with the highest concentration on their outside edge (arrows). (**c**, **d**) There are receptors with a single large and thick cilium (arrows)—presumably mechanoreceptors of type 2. Next to them, there are also numerous receptors with a thin long cilium (type 3). Scale bars: (**a**) 50 μm; (**b**, **c**) 20 μm; (**d**) 10 μm

organs, numerous muscle fibers (Figs. 7, 8, 16, 17 and 18), and even individual neurons (Fig. 17). *See also* **Note 4**.

4 Notes

1. We attempted to fix six different species of ctenophores for SEM microscopy. It is important to note that adult animals from *Bolinopsis* and *Mnemiopsis* genera could not be fixed in glutaraldehyde. They dissolved in the fixative, with cells losing connection to each other and their tissue losing its integrity. These two species have some of the most fragile and full of water bodies among ctenophores, and we found them inappropriate for SEM investigation. Animals from four other genera—*Pleurobrachia*, *Beroe*, *Euplokamis*, and *Hormiphora*—have much tougher bodies and demonstrated good fixation

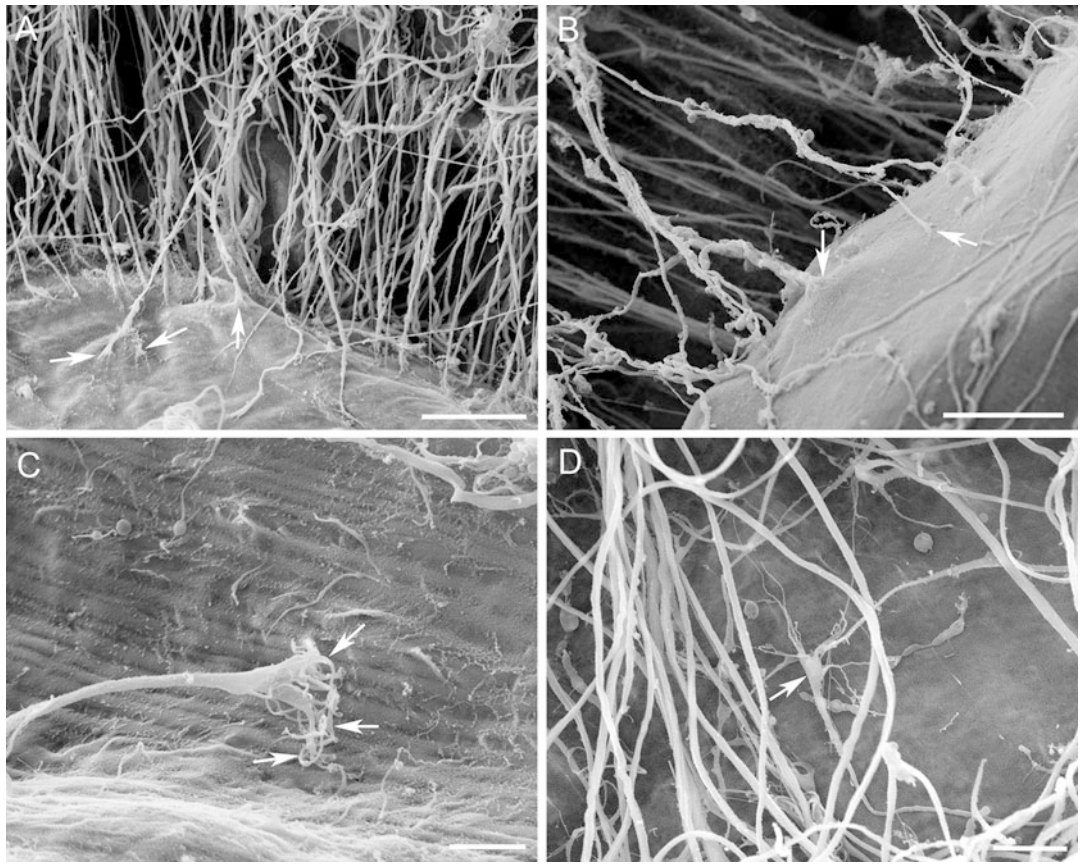

Fig. 16 Muscle fibers in the mesoglea of *Pleurobrachia*. (**a**, **b**) Many mesogleal muscle fibers are firmly attached to the surface of the pharynx (arrows indicate the attachment point) and well preserved after the drying process. (**c**) There is always some branching and widening of the muscle fiber at the point of contact to increase the binding surface (arrows). (**d**) Mesogleal neuronal-like processes (arrow) with extensive branching are among muscle fibers on the surface of the pharynx. Scale bars: (**a**, **b**) 50 μm; (**c**) 10 μm; (**d**) 20 μm

results. Most SEM research was done on *Pleurobrachia bachei* and *Beroe abyssicola* [25–27].

2. The primary fixative, 2.5% glutaraldehyde, could be prepared in 0.1 M cacodylate buffer (prepared from sodium cacodylate in distilled water). In this case, the subsequent washing steps also should be carried in 0.1 M cacodylate buffer, and 4% osmium tetroxide should be diluted in 0.2 M cacodylate buffer at 1:1 ratio. Both PBS and cacodylate buffer gave very good fixation results for SEM. Cacodylate buffer has both positive and negative sides. The negative side is its toxicity and carcinogenic effects. One must be cautious during pH adjustment by adding HCl—it causes the release of arsenic and should be processed under a hood and while wearing gloves. The positive side is resistance to bacterial contamination and the ability to store samples for long periods of time.

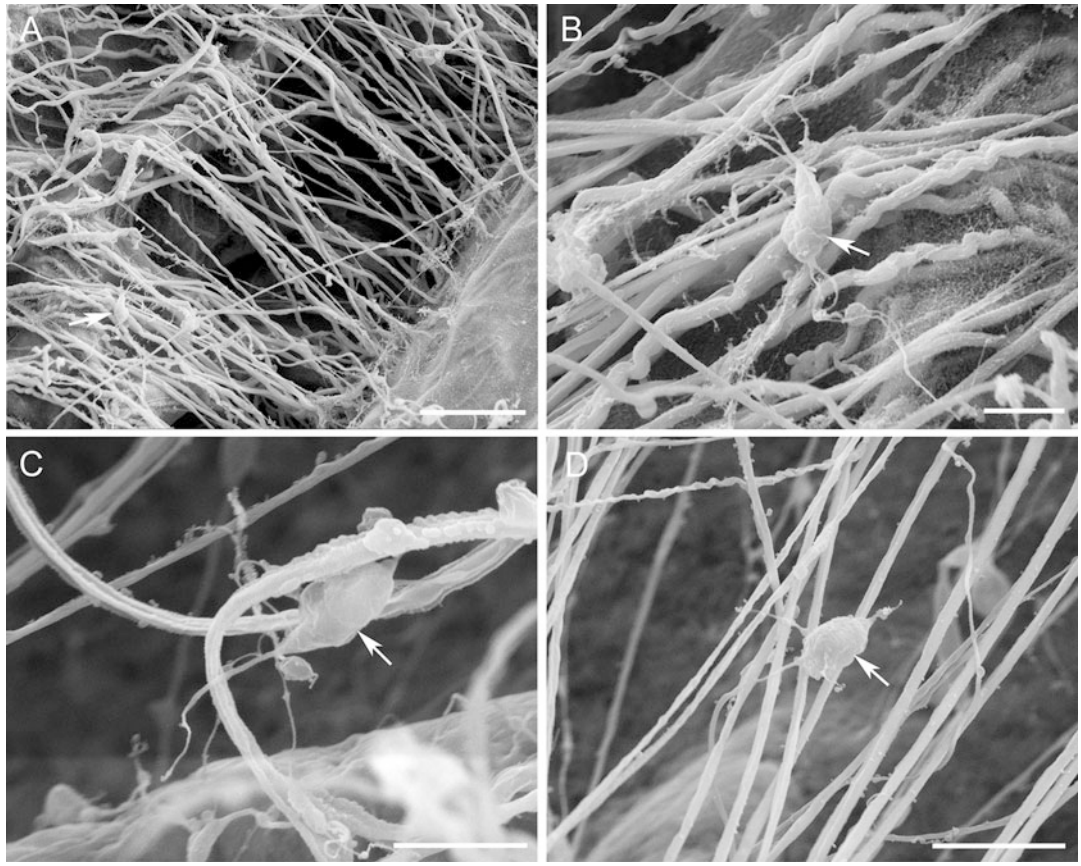

Fig. 17 Mesogleal neural-like cells (arrows) among muscle fibers in the pharynx area of *Pleurobrachia*. Scale bars: (**a**) 50 μm; (**b**, **c**) 10 μm; (**d**) 20 μm

3. There are several possible ways of drying tissue for SEM. Some insects with their hard exoskeleton, fish scales, or teeth of mammals and other vertebrates, etc., do not require any special drying technique or even dehydration—just a simple air drying would suffice. However, for most soft-bodied animals, tissue drying is crucial for SEM. Critical point drying is the most common method of drying biological specimens for SEM. The regular air drying of biological specimens can cause severe deformation of the surface structure due to the considerable surface tension present at the phase boundary as the liquid evaporates. Water, for example, has a very high surface tension to air. During critical point drying, this surface tension is reduced to zero. It is achieved by choosing a specific temperature and pressure for suitable inert fluid (liquid CO_2 is universally used today) along the boundary between the liquid and gaseous phases, where liquid and vapor have the same density— the critical point. For CO_2, the critical point is achieved at 35 °C and 1200 psi. When the temperature is raised

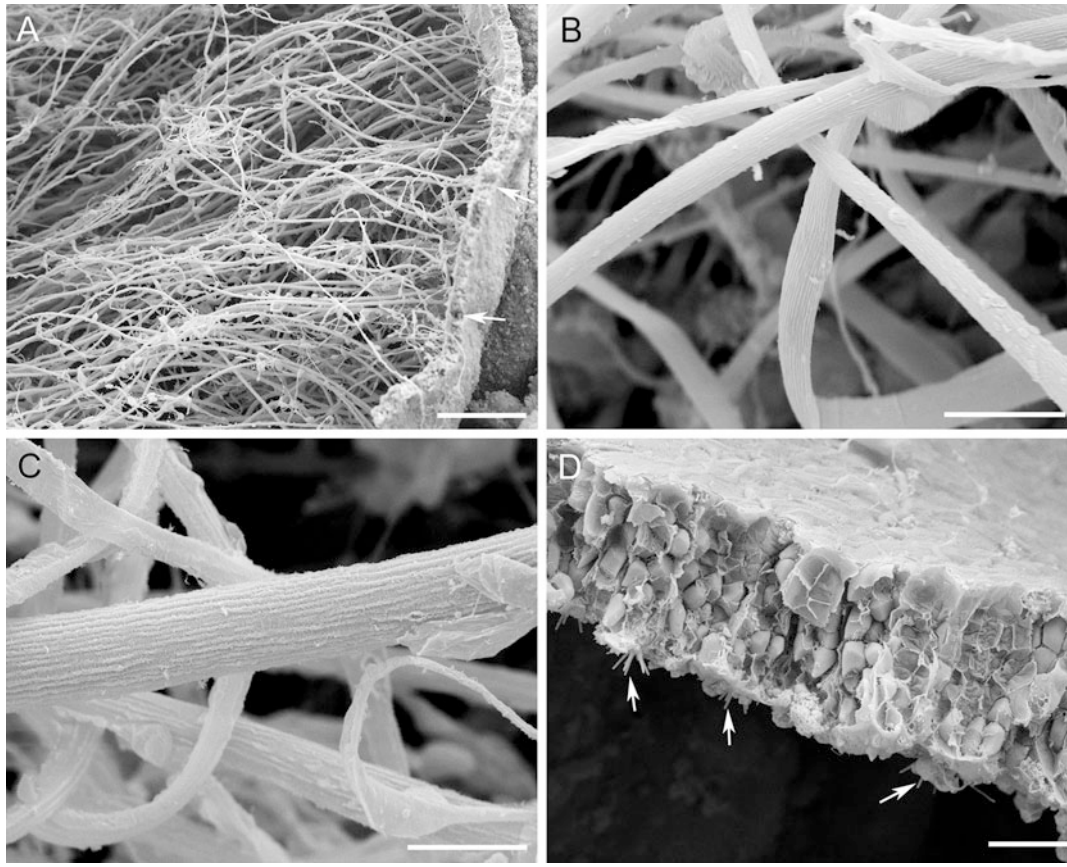

Fig. 18 Mesogleal muscles in *Beroe*. (**a**) The body wall (arrows) is broken open to reveal dense muscle fibers inside the mesogleal area. (**b**, **c**) Long muscle fibers have a variable thickness. (**d**) A glimpse at the cross-section of the body wall. Note the receptors with multiple cilia (arrows) located on the outer surface of the body. Scale bars: (**a**) 100 μm; (**b**) 20 μm; (**c**, **d**) 10 μm

above the critical temperature, liquid CO_2 changes to vapor without a change of density and no surface tension and, therefore, completely preserves the surface structure of the tissue.

In addition to the critical point drying technique, the chemical drying procedure has been successfully used for some biological specimens. One example is the use of hexamethyldisilazane (HMDS), which has been described as a good alternative. After dehydration, ethanol is replaced with HMDS, and the tissue is then left under the hood for complete air drying. The surface tension for HMDS during evaporation is much smaller than for water, and therefore, preservation of the surface structure is much better. We tried to use HMDS with our ctenophore samples as a much simpler alternative but found that the preparation quality was significantly lower than after the critical point drying. Therefore, the decision

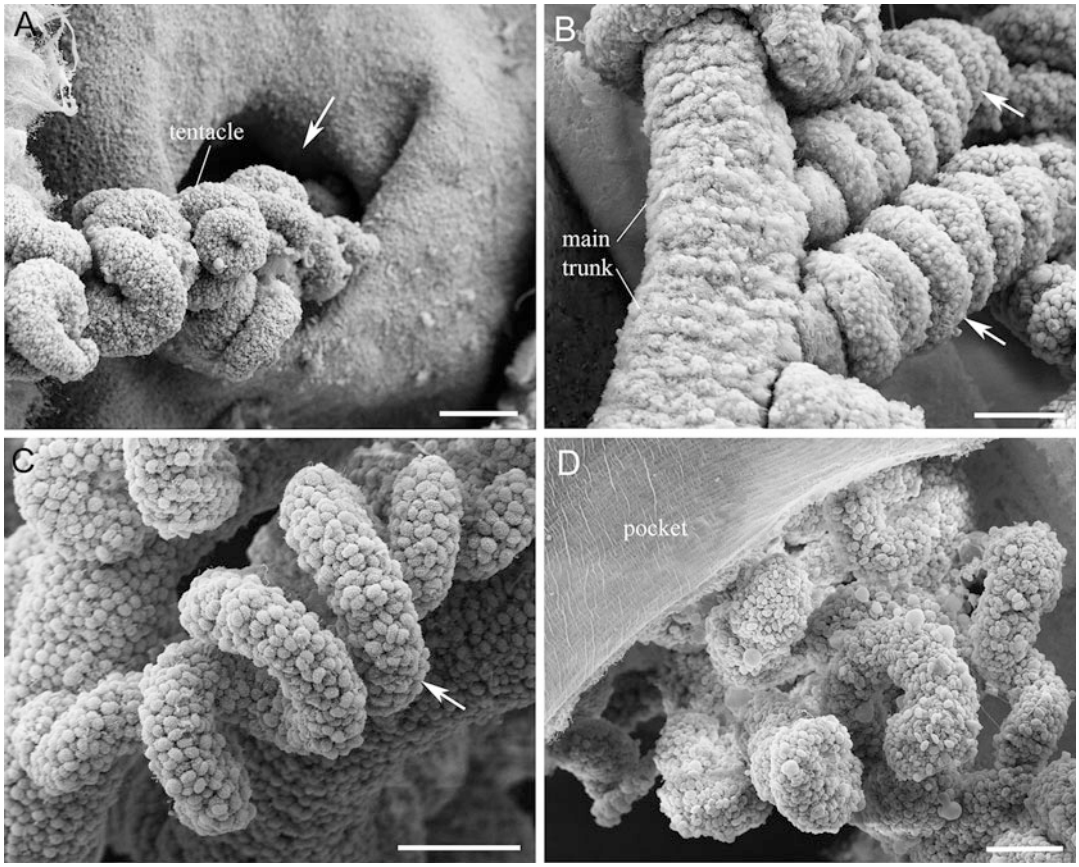

Fig. 19 Tentacles in adult *Pleurobrachia*. (**a**) Tentacle protruding from the opening of the tentacle pocket (arrow). (**b**, **c**) Each tentacle consists of the main trunk and secondary tentacles packed in tight spirals (arrows). Small round-shaped colloblasts are visible along the main trunk and secondary tentacles. (**d**) The tentacle pocket is cut open and shows a withdrawn tentacle inside. Scale bars: (**a**) 100 μm; (**b**, **c**, **d**) 50 μm

has been made to use only critical point drying with ctenophores.

4. We used SEM to analyze not only the tissue of adult ctenophores but also looked at the *Pleurobrachia* embryos during different stages of their development [25]. The basic protocol for processing embryos is very similar to that of adult animals. There are only two details that should be stressed here. Embryos are very small and, most of the time, are suspended in the water column, making it very difficult to rinse them and change solutions. So, we used for that purpose the 2 mL Eppendorf tubes and centrifuge to separate them from a liquid (500 rotations per minute for live embryos and 1000 rotations per minute for fixed embryos for 2–3 min) and then change solutions multiple times. Also, it is necessary to have a large number of embryos fixed initially because many of them will be lost during processing (up to 30–40% of the original number).

Another challenging detail—scanning embryos of the very early stages. *Pleurobrachia* embryos hatch on approximately the third day. To look at one-day or two-day-old embryos, it is necessary to remove them from the egg by fine forceps under the dissecting scope (Fig. 2a). Otherwise, the eggshell is not penetrable for SEM electrons. It is a very time-consuming work. However, after hatching on day 3, this problem does not exist (Fig. 2b).

Acknowledgments

This work was supported in part by the Human Frontiers Science Program (RGP0060/2017) and the National Science Foundation (IOS-1557923) grants to LLM. Research reported in this publication was also supported in part by the National Institute of Neurological Disorders and Stroke of the National Institutes of Health under award number R01NS114491 (to LLM). The content is solely the authors' responsibility and does not necessarily represent the official views of the National Institutes of Health.

References

1. Horridge GA (1964) The giant mitochondria of ctenophore comb plates. Q J Microsc Sci 105:301–310
2. Horridge GA (1964) Presumed photoreceptive cilia in a ctenophore. Q J Microsc Sci 105:311–317
3. Horridge GA (1965) Non-motile sensory cilia and neuromuscular junctions in a ctenophore independent effector organ. Proc R Soc Lond Biol 162:333–350
4. Horridge GA (1974) Recent studies on the Ctenophora. In: Muscatine L, Lenhoff HM (eds) Coelenterate biology. Academic, New York, pp 439–468
5. Horridge GA, Mackay B (1964) Neurociliary synapses in *Pleurobrachia* (Ctenophora). Q J Microsc Sci 105:163–174
6. Horridge GA, Tamm SL (1969) Critical point drying for scanning electron microscopic sthdy of ciliary motion. Science 163(3869):817–818
7. Hernandez-Nicaise M-L (1991) Ctenophora. In: Harrison FWFW, Westfall JA (eds) Microscopic anatomy of invertebrates: Placozoa, Porifera, Cnidaria, and Ctenophora. Wiley, New York, pp 359–418
8. Hernandez-Nicaise ML (1973) The nervous system of ctenophores. II. The nervous elements of the mesoglea of beroids and cydippids (author's transl). Z Zellforsch Mikrosk Anat 143(1):117–133
9. Hernandez-Nicaise ML (1973) The nervous system of ctenophores. I. Structure and ultrastructure of the epithelial nerve-nets. Z Zellforsch Mikrosk Anat 137(2):223–250
10. Hernandez-Nicaise ML (1973) The nervous system of ctenophores. III. Ultrastructure of synapses. J Neurocytol 2(3):249–263
11. Hernandez-Nicaise ML, Amsellem J (1980) Ultrastructure of the giant smooth muscle fiber of the ctenophore *Beroe ovata*. J Ultrastruct Res 72(2):151–168
12. Tamm SL (1982) Ctenophora. In: Electrical conduction and behavior in "simple" invertebrates. Clarendon Press, Oxford, pp 266–358
13. Tamm SL (2014) Cilia and the life of ctenophores. Invertebr Biol 133(1):1–46
14. Halanych KM et al (2016) Miscues misplace sponges. Proc Natl Acad Sci U S A 113(8): E946–E947
15. Li Y et al (2021) Rooting the animal tree of life. Mol Biol Evol 38(10):4322–4333
16. Redmond AK, McLysaght A (2021) Evidence for sponges as sister to all other animals from partitioned phylogenomics with mixture models and recoding. Nat Commun 12(1):1783

17. Telford MJ, Moroz LL, Halanych KM (2016) Evolution: a sisterly dispute. Nature 529(7586):286–287
18. Whelan NV et al (2017) Ctenophore relationships and their placement as the sister group to all other animals. Nat Ecol Evol 1(11): 1737–1746
19. Moroz LL (2015) Convergent evolution of neural systems in ctenophores. J Exp Biol 218 (Pt 4):598–611
20. Moroz LL et al (2014) The ctenophore genome and the evolutionary origins of neural systems. Nature 510(7503):109–114
21. Moroz LL, Kohn AB (2016) Independent origins of neurons and synapses: insights from ctenophores. Philos Trans R Soc Lond Ser B Biol Sci 371(1685):20150041
22. Moroz LL (2014) The genealogy of genealogy of neurons. Commun Integr Biol 7(6): e993269
23. Moroz LL, Romanova DY, Kohn AB (1821) Neural versus alternative integrative systems: molecular insights into origins of neurotransmitters. Philos Trans R Soc Lond Ser B Biol Sci 2021(376):20190762
24. Sebe-Pedros A et al (2018) Early metazoan cell type diversity and the evolution of multicellular gene regulation. Nat Ecol Evol 2(7): 1176–1188
25. Norekian TP, Moroz LL (2016) Development of neuromuscular organization in the ctenophore *Pleurobrachia bachei*. J Comp Neurol 524(1):136–151
26. Norekian TP, Moroz LL (2019) Neural system and receptor diversity in the ctenophore *Beroe abyssicola*. J Comp Neurol 527(12): 1986–2008
27. Norekian TP, Moroz LL (2019) Neuromuscular organization of the Ctenophore *Pleurobrachia bachei*. J Comp Neurol 527(2):406–436
28. Norekian TP, Moroz LL (2020) Atlas of the neuromuscular system in the Trachymedusa *Aglantha digitale*: insights from the advanced hydrozoan. J Comp Neurol 528(7): 1231–1254